High Order Vectorial Analysis of Waveguides With Curved Dielectric Interfaces

Shan Zhao

***Abstract*—This letter introduces a novel full vectorial higher order finite difference method for the modal analysis of optical waveguides with smoothly curved dielectric interfaces. Based on a simple Cartesian grid, a new matched interface and boundary formulation is derived to enforce the interface conditions so that the staircasing error can be eliminated. Benchmark problems are employed to validate the proposed method. A fourth order convergence is numerically confirmed irrespective of the presence of the step-index interfaces.**

***Index Terms*—Eigenvalues and eigenfunctions, finite difference methods, nonhomogeneous media, waveguide theory.**

I. Introduction

In recent years, there has been an increased interest in the design of optoelectronic devices with non-rectangular cross sections to address various application needs. To model arbitrarily curved dielectric interfaces with more accuracy, one popular way in the literature is fitting the grid to the boundaries. For example, a nonuniform triangular mesh has been adopted in a full vectorial finite difference (FD) method for this purpose [1], while some advanced finite element methods [2], [3] employ curvilinear/isoparametric elements to achieve a better fit. Within the boundary integral framework, curved interfaces are suggested to be represented via a combination of circular and elliptical segments [4]. The method of lines analysis has been extended to deal with arbitrarily curved interfaces in [5]. By only discretizing on the interfaces, the boundary element method (BEM) is naturally suited for curved interface problems. A full vectorial BEM has been introduced to produce highly accurate results [6]. In general, the success of the aforementioned methods essentially lies in the use of body-fitted grids so that the staircasing error can be avoided.

It is well known that across dielectric interfaces, field components are nonsmooth or even discontinuous [7]. Thus, to achieve a higher order accuracy, special interface treatments in which the interface conditions are properly imposed in the discretization, are indispensable. For rectangular waveguides, such interface treatments have achieved a great success, giving rise to up to 12th order FD interface schemes [8]–[11]. Second order interface schemes have also been constructed for waveguides with curved interfaces [12], [13]. Based on a simple Cartesian grid, the enforcement of interface conditions in some sense fits the differencing weights to the dielectric interfaces so that the staircasing error is eliminated.

Manuscript received November 19, 2008; revised February 15, 2009. First published April 24, 2009; current version published May 08, 2009. This work was supported in part by the National Science Foundation (NSF) under Grants DMS-0616704 and DMS-0731503.

The author is with the Department of Mathematics, University of Alabama, Tuscaloosa, AL 35487 USA (e-mail: szhao@bama.ua.edu).

Color versions of one or more of the figures in this letter are available online at http://ieeexplore.ieee.org.

Digital Object Identifier 10.1109/LMWC.2009.2017584

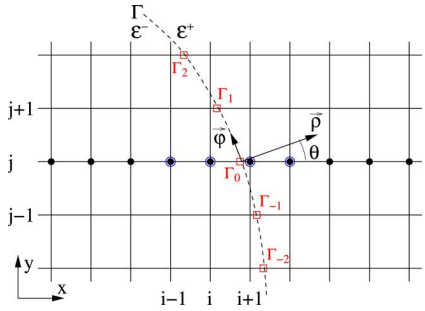

Fig. 1. Illustration of the MIB grid partition. Filled circles: Cartesian nodes; Open circles: fictitious nodes; Squares: auxiliary nodes.

The objective of this Letter is to introduce a fourth order full-vectorial matched interface and boundary (MIB) method for optical waveguides with smoothly curved interfaces. The MIB was first proposed for solving Maxwell's equations with straight interfaces [7], and it has been generalized to treat curved interfaces for solving the scalar Poisson equation [14]. The MIB has also been reformulated to impose complex boundary conditions for general boundary value problems and initial-boundary value problems in [15]. Recently, a full-vectorial MIB method has been constructed for solving rectangular optical waveguides with straight interfaces [11].

II. Formulation and Discretization

Consider a step-index optical waveguide with smoothly curved interfaces. A full vectorial formulation in terms of transverse magnetic field components H^x and H^y will be constructed based on a simple Cartesian grid. A typical local configuration is shown in Fig. 1. Except on interface Γ, both H^x and H^y satisfy the scalar Helmholtz equation

$$\frac{\partial^2 H}{\partial x^2} + \frac{\partial^2 H}{\partial y^2} + k_0^2 \epsilon H = \beta^2 H \tag{1}$$

where $H = H^x$ or $H = H^y$, β is the propagation constant, ϵ is the relative permittivity coefficient, $k_0 = 2\pi/\lambda$ is the free space wavenumber with λ being the free space wavelength.

Away from Γ, the standard fourth order finite difference (FD) discretization of (1) is carried out, while the FD weights of nodes in the vicinity of the interface shall be modified. A universal rule here is that to approximate function or its derivatives on one side of interface, one never *directly* refers to function values from the other side. Instead, in the MIB scheme [7], [11], [14], [15], fictitious values from the other side of the interface will be used. For example, referring to Fig. 1, we denote $H_{i,j}$ and

$\tilde{H}_{i,j}$, respectively, to be function and fictitious value at the node (x_i, y_j). The fourth order FD approximation near the interface will be modified to be

$$\frac{\partial^2}{\partial x^2}H_{i,j} = \frac{1}{\Delta x^2}\Big(-\frac{1}{12}H_{i-2,j} + \frac{4}{3}H_{i-1,j} - \frac{5}{2}H_{i,j} + \frac{4}{3}\tilde{H}_{i+1,j} - \frac{1}{12}\tilde{H}_{i+2,j}\Big). \quad (2)$$

This calls for accurate generation of four layers of fictitious values $\tilde{H}$ (marked with open circles in Fig. 1) surrounding Γ, two inside and two outside.

Consider the MIB interface treatment along x direction, see Fig. 1. The MIB scheme for y direction can be similarly formulated. Eight fictitious values of $\tilde{H}^x$ and $\tilde{H}^y$ on four fictitious points (x_{i-1}, y_j), (x_i, y_j), (x_{i+1}, y_j), and (x_{i+2}, y_j) need to be determined. This will be achieved via iteratively solving jump conditions at the interface point (Γ_0, y_j). These physical jump conditions are defined on a local cylindrical coordinate system $(\vec{\rho}, \vec{\varphi}, \vec{z})$ (see Fig. 1). Let the curvature of the interface at (Γ_0, y_j) be κ or the effective radius be $R = 1/\kappa$. We denote a function jump at point (Γ_0, y_j) to be $[H] := \lim_{\rho\to R^+} H - \lim_{\rho\to R^-} H$. We have totally six jump conditions available [12]

$$[H^\rho] = 0,\ [H^\varphi] = 0,\ \left[\frac{\partial H^\rho}{\partial \rho}\right] = 0,\ \left[\frac{\partial H^\rho}{\partial \varphi}\right] = 0 \quad (3)$$

$$\left[\frac{\partial H^\varphi}{\partial \varphi}\right] = 0,\ \left[\frac{1}{\epsilon}\frac{\partial H^\varphi}{\partial \rho}\right] + \frac{1}{R}\left[\frac{1}{\epsilon}H^\varphi\right] = \frac{1}{R}\left[\frac{1}{\epsilon}\frac{\partial H^\rho}{\partial \varphi}\right]. \quad (4)$$

We note that the previously developed MIB method [11] is not able to handle the current situation because the jump conditions are in terms of local field components (H^ρ, H^φ).

A new full vectorial MIB method will be constructed, which involves both a global Cartesian coordinate and local coordinates for each interface matching. In particular, the Helmholtz (1) will be solved throughout for (H^x, H^y), while jump conditions (3) and (4) will be discretized in terms of (H^ρ, H^φ). A local coordinate transformation will be employed to convert between them. Referring to Fig. 1, we denote the angle between x direction and radial direction at point (Γ_0, y_j), i.e., $\vec{\rho}$, to be θ. Then the forward and backward transforms are given as

$$H^\rho = \cos\theta H^x + \sin\theta H^y,\ H^\varphi = -\sin\theta H^x + \cos\theta H^y \quad (5)$$

$$H^x = \cos\theta H^\rho - \sin\theta H^\varphi,\ H^y = \sin\theta H^\rho + \cos\theta H^\varphi. \quad (6)$$

To avoid unnecessary interpolations, jump conditions (3) and (4) will be discretized on the global Cartesian nodes as shown in Fig. 1. We thus need to rewrite jump conditions (3) and (4) into Cartesian directions (x, y). Consider H^ρ first. Conditions $[\partial H^\rho/\partial\rho] = 0$ and $[\partial H^\rho/\partial\varphi] = 0$ give rise to $[\partial H^\rho/\partial x] = 0$ and $[\partial H^\rho/\partial y] = 0$. This means that the MIB treatment of H^ρ can be carried out in a dimension-by-dimension manner.

For the interface topology shown in Fig. 1, MIB interface matching of H^ρ should naturally be conducted along x direction. We will determine four fictitious nodes as shown in Fig. 1 by discretizing the following two jump conditions:

$$[H^\rho] = 0, \quad \left[\frac{\partial H^\rho}{\partial x}\right] = 0. \quad (7)$$

To this end, an iterative procedure is employed in the MIB scheme [7], [11], [14], [15]. At the first step, we determine two fictitious values $\tilde{H}^\rho_{i,j}$ and $\tilde{H}^\rho_{i+1,j}$ by discretizing (7) based on two grid stencils, i.e., $\mathbf{H}^-_\rho := (H^\rho_{i-4,j}, H^\rho_{i-3,j}, H^\rho_{i-2,j}, H^\rho_{i-1,j}, H^\rho_{i,j}, \tilde{H}^\rho_{i+1,j})^T$ and $\mathbf{H}^+_\rho := (\tilde{H}^\rho_{i,j}, H^\rho_{i+1,j}, H^\rho_{i+2,j}, H^\rho_{i+3,j}, H^\rho_{i+4,j}, H^\rho_{i+5,j})^T$. Denote the finite difference (FD) weight vector of these two stencils differentiating at Γ_0 to be, respectively, $\mathbf{W}^-_k$ and $\mathbf{W}^+_k$. Here the subscript k represents interpolation $(k = 0)$ and the first order derivative approximation $(k = 1)$. Then, (7) becomes

$$\mathbf{W}^-_0\mathbf{H}^-_\rho = \mathbf{W}^+_0\mathbf{H}^+_\rho, \quad \mathbf{W}^-_1\mathbf{H}^-_\rho = \mathbf{W}^+_1\mathbf{H}^+_\rho. \quad (8)$$

By solving (8), one attains $\tilde{H}^\rho_{i,j}$ and $\tilde{H}^\rho_{i+1,j}$. At the next step, we redefine each stencil by introducing one more fictitious point $\mathbf{H}^-_\rho := (H^\rho_{i-4,j}, \ldots, H^\rho_{i,j}, \tilde{H}^\rho_{i+1,j}, \tilde{H}^\rho_{i+2,j})^T$ and $\mathbf{H}^+_\rho := (\tilde{H}^\rho_{i-1,j}, \tilde{H}^\rho_{i,j}, H^\rho_{i+1,j}, \ldots, H^\rho_{i+5,j})^T$. Consequently, $\mathbf{W}^-_k$ and $\mathbf{W}^+_k$ will also be re-calculated. Then, two more fictitious values $\tilde{H}^\rho_{i-1,j}$ and $\tilde{H}^\rho_{i+2,j}$ can be solved from (8), since $\tilde{H}^\rho_{i,j}$ and $\tilde{H}^\rho_{i+1,j}$ are now known. This gives four layers of $\tilde{H}^\rho$ fictitious values.

We next discuss the MIB treatment for H^φ. We first rewrite jump conditions (4) into one that involves x and φ derivatives,

$$\left[\frac{1}{\epsilon}\frac{\partial H^\varphi}{\partial x}\right] + \frac{\sin\theta}{R}\left[\frac{1}{\epsilon}\frac{\partial H^\varphi}{\partial \varphi}\right] = \frac{\cos\theta}{R}\left(\left[\frac{1}{\epsilon}\frac{\partial H^\rho}{\partial \varphi}\right] - \left[\frac{1}{\epsilon}H^\varphi\right]\right). \quad (9)$$

Two Cartesian terms in (9), i.e., $[1/\epsilon\partial H^\varphi/\partial x]$ and $[1/\epsilon H^\varphi]$ can be discretized as in (8). For example, by similarly defining $\mathbf{H}^-_\varphi$ and $\mathbf{H}^+_\varphi$, we have $[1/\epsilon\partial H^\varphi/\partial x] = 1/\epsilon^+\mathbf{W}^+_1\mathbf{H}^+_\varphi - 1/\epsilon^-\mathbf{W}^-_1\mathbf{H}^-_\varphi$. The other two terms of (9) involve φ derivatives. Moreover, these φ derivatives are continuous across the interface, according to the jump conditions $[\partial H^\rho/\partial\varphi] = 0$ and $[\partial H^\varphi/\partial\varphi] = 0$. Thus, we have $[1/\epsilon\partial H^\varphi/\partial\varphi] = [1/\epsilon]\partial H^\varphi/\partial\varphi = (1/\epsilon^+ - 1/\epsilon^-)\partial H^\varphi/\partial\varphi$ and $[1/\epsilon\partial H^\rho/\partial\varphi] = [1/\epsilon]\partial H^\rho/\partial\varphi = (1/\epsilon^+ - 1/\epsilon^-)\partial H^\rho/\partial\varphi$. In other words, these two terms need not be discretized by means of two stencils from both sides of the interface. Instead, they will be discretized along the interface. Denote some auxiliary points to be intersection points of the interface Γ with x grid lines, i.e., (Γ_{-2}, y_{j-2}), (Γ_{-1}, y_{j-1}), (Γ_0, y_j), (Γ_1, y_{j+1}), and (Γ_2, y_{j+2}) in Fig. 1. A five points stencil FD weight vector $\mathbf{W}^\Gamma_k$ will be used to discretize these φ derivatives. Let the corresponding vectors of auxiliary values to be $\mathbf{H}^\Gamma_\rho$ and $\mathbf{H}^\Gamma_\varphi$. The first order jump condition (9) will be discretized as

$$\frac{1}{\epsilon^+}\left(\mathbf{W}^+_1 + \frac{\cos\theta}{R}\mathbf{W}^+_0\right)\mathbf{H}^+_\varphi + \frac{\sin\theta}{R}\left[\frac{1}{\epsilon}\right]\mathbf{W}^\Gamma_1\mathbf{H}^\Gamma_\varphi = \frac{1}{\epsilon^-}\left(\mathbf{W}^-_1 + \frac{\cos\theta}{R}\mathbf{W}^-_0\right)\mathbf{H}^-_\varphi + \frac{\cos\theta}{R}\left[\frac{1}{\epsilon}\right]\mathbf{W}^\Gamma_1\mathbf{H}^\Gamma_\rho. \quad (10)$$

The zeroth order jump condition $[H^\varphi] = 0$ will be discretized as in (8). Then a two step procedure as in the H^ρ case will be employed to estimate four $\tilde{H}^\varphi$ fictitious values.

The MIB scheme discussed above will essentially represent four layers of $\tilde{H}^\rho$ and $\tilde{H}^\varphi$ in terms of H^ρ and H^φ values on a set of 15 nodes (10 along x line and 5 auxiliary points). Via the coordinate transformations (5) and (6), each fictitious value of $\tilde{H}^x$ or $\tilde{H}^y$ is also a linear combination of 30 function values of H^x and H^y on 15 nodes. Finally, to attain a full Cartesian grid approach, each auxiliary point will be interpolated along x line by using five nearest nodes exclusively inside the interface.

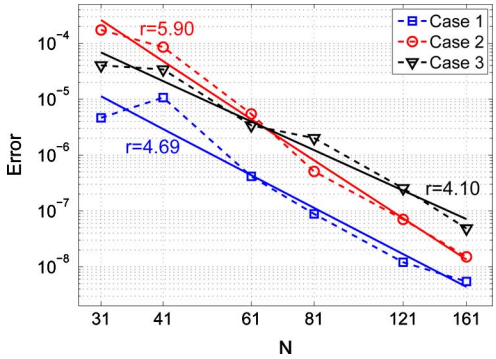

Fig. 2. Numerical convergence tests of the MIB scheme.

Therefore, in the final MIB discretization, each fictitious value of $\hat{H}^x$ or $\hat{H}^y$ will depend on totally 60 function values on 30 Cartesian nodes.

III. Numerical Results

To validate the proposed full vectorial MIB approach, we consider three benchmark tests of step-index fibers with different refractive index n and wavelength λ[1], [6]. The core radius of the fiber is fixed to be $4\ \mu\mathrm{m}$, while other three parameters $(n_{\mathrm{core}}, n_{\mathrm{clad}}, \lambda)$ are given as, respectively, (1.45,1.44,1.55), (1.5,1.0,6.2), and (3.5,1.0,6.2) in case 1, 2, and 3. We will calculate the fundamental HE_{11} mode and compare with the analytical solutions [1], [6]. The analytical effective propagation constant $\beta_e = \beta/k$ is given to be 1.44607 67348 5869, 1.40948 36877 8245, and 3.45285 49556 2367, respectively, for case 1, 2, and 3.

For each case, a large enough square computational domain $[-a, a] \times [-a, a]$ with Dirichlet zero boundary conditions will be used. A uniform mesh of size $N \times N$, i.e., $\Delta x = \Delta y$, is employed in all cases. In [1], by exploiting the symmetry, only a one-quarter of region is discretized. In the present study, in order to test the performance of the proposed MIB method, it is desired that the interface intersection and orientation with respect to the Cartesian grid could be arbitrary. Thus, the entire domain will be discretized and the domain dimension a will be chosen as a non-integer number. In particular, a is selected to be $10 + \pi/3$ for case 1 and 2, and $5 + \pi/3$ for case 3.

The absolute errors of the MIB scheme are depicted as dashed lines in Fig. 2. To analyze the numerical convergence rate r of the MIB scheme, a linear fitting by means of the least squares is conducted in the log-log scale [11]. The resulting solid convergence line and the corresponding slope are also shown in Fig. 2. For case 1, 2, and 3, the numerical order r is calculated to be 4.69, 5.90, and 4.10. This verifies the fourth order convergence of the MIB scheme and the present results are significantly more accurate than those reported in [1] and [6]. Among three cases, the best accuracy is achieved in the case 1, because a weakly guided structure is solved there. The over-performance rate 5.90 of the case 2 should be due to the impaired MIB accuracies for $N \leq 61$. Such an accuracy reduction on coarse grids might be due to the fact that there are limited nodes inside the fiber, while this is not an issue for the case 3 thanks to a smaller a.

We note that the CPU time consumed for solving each fictitious value is independent of N. The computational overhead of the MIB treatments essentially scales as $O(N)$, since the number of total irregular points is one dimension lower than the number of total grid points. In the present experiments, the MIB preprocessing usually takes less than 1% CPU time.

IV. Conclusion

In summary, we have introduced a novel full vectorial MIB method for solving optical waveguides with smoothly curved interfaces. Compared with the previously developed MIB method for rectangular waveguides [11], the current approach overcomes a major difficulty in relating a global Cartesian grid with different local cylindrical coordinates at different interface points. A fourth order convergences is reported for the first time in the literature for the benchmark problems of step-index fibers. The testing of the proposed MIB method for more complex interfaces is currently under investigation. We finally note that the proposed method is designed for smoothly curved interfaces, i.e., C^1 continuous interfaces. If the interface is C^0, certain corner singularity problems may occur so that the fourth order convergence might not be guaranteed [9]–[11].

References

[1] G. R. Hadley, "Numerical simulation of waveguides of arbitrary cross section," *Int. J. Electron. Common.*, vol. 58, pp. 86–92, 2004.
[2] M. Koshiba and Y. Tsuji, "Curvilinear hybrid edge/nodal elements with triangular shape for guide-wave problems," *J. Lightwave Tech.*, vol. 18, pp. 737–743, 2000.
[3] K. Dossou and M. Fontaine, "A high order isoparametric finite element method for the computation of waveguide modes," *Comput. Method Appl. Mech. Eng.*, vol. 194, pp. 837–858, 2005.
[4] S. Cogollos, S. Marini, V. E. Boria, P. Soto, A. Vidal, H. Esteban, J. V. Morro, and B. Gimeno, "Efficient model analysis of arbitrarily shaped waveguides composed of linear, circular, and elliptical arcs using the bi-RME method," *IEEE Trans. Microw. Theory Tech.*, vol. 51, no. 12, pp. 2378–2390, Dec. 2003.
[5] W. D. Yang and R. Pregla, "The method of lines for analysis of integrated optical waveguide structures with arbitrary curved interfaces," *J. Lightwave Tech.*, vol. 14, pp. 879–884, 1996.
[6] T. Lu and D. Yevick, "A vectorial boundary element method analysis of integrated optical waveguides," *J. Lightwave Tech.*, vol. 21, pp. 1793–1807, 2003.
[7] S. Zhao and G. W. Wei, "High-order FDTD methods via derivative matching for Maxwell's equations with material interfaces," *J. Comput. Phys.*, vol. 200, pp. 60–103, 2004.
[8] G. R. Hadley, "High-accuracy finite-difference equations for dielectric waveguide analysis I: Uniform regions and dielectric interfaces," *J. Lightwave Tech.*, vol. 20, pp. 1210–1218, 2002.
[9] G. R. Hadley, "High-accuracy finite-difference equations for dielectric waveguide analysis II: Dielectric corners," *J. Lightwave Tech.*, vol. 20, pp. 1219–1231, 2002.
[10] N. Thomas, P. Sewell, and T. M. Benson, "A new full-vectorial higher order finite-difference scheme for the modal analysis of rectangular dielectric waveguides," *J. Lightwave Tech.*, vol. 25, pp. 2563–2570, 2007.
[11] S. Zhao, "Full-vectorial matched interface and boundary (MIB) method for the modal analysis of dielectric waveguides," *J. Lightwave Tech.*, vol. 26, pp. 2251–2259, 2008.
[12] Y. C. Chiang, Y. P. Chiou, and H. C. Chang, "Improved full-vectorial finite-difference mode solver for optical waveguides with step-index profiles," *J. Lightwave Tech.*, vol. 20, pp. 1609–1618, 2002.
[13] T. P. Horikis and W. L. Kath, "Modal analysis of circular bragg fibers with arbitrary index profiles," *Opt. Let.*, vol. 31, pp. 3417–3419, 2006.
[14] Y. C. Zhou, S. Z. M. Feig, and G. W. Wei, "High order matched interface and boundary (MIB) schemes for elliptic equations with discontinuous coefficients and singular sources," *J. Comput. Phys.*, vol. 213, pp. 1–30, 2006.
[15] S. Zhao and G. W. Wei, "Matched interface and boundary (MIB) method for the implementation of boundary conditions in high-order central finite differences," *Int. J. Numer. Method Eng.*, vol. 77, no. 12, pp. 1690–1730, Sep. 2009.